A Preliminary Directional Study of Cosmic Rays at High Altitude.* II. Experimental Results and Interpretation

J. R. WINCKLER AND W. G. STROUD
Appendix by T. J. B. SHANLEY
Palmer Physical Laboratory, Princeton University, Princeton, New Jersey
(Received June 9, 1949)

The zenithal distribution of particles at high altitudes observed with counter telescopes has been compared with simple calculations concerning the multiplicity and angular divergence of secondary particles. The observations are in agreement with a sharply collimated forward type of production event, and disagree with the wide angle type of production of hard secondaries. The azimuthal distributions and zenithal distributions indicate a nearly isotropic primary flux, in agreement with geomagnetic considerations at geonetic latitude 56°N. The effects of the atmosphere on directional asymmetry measurements at 13-g/cm² atmospheric depths are concluded to be small, especially if lead filters of a few cm thickness are used. The number of low energy particles is small at this depth.

I. EXPERIMENTAL RESULTS

THE data obtained in the series of experiments described in the previous paper may be presented in four ways:

(1) Counting rate *vs.* atmospheric depth for various lead filter thicknesses at each zenith angle (average of all azimuths).
(2) The zenithal distribution for various filter thicknesses at several atmospheric depths (average of all azimuths).
(3) The integrated flux at various atmospheric depths.
(4) The azimuthal distribution (successfully measured for 45°, 67°, and 90° with 7.6 cm-lead filter only at approximately 1.5 cm Hg pressure).

The curves in category (1) are shown in Fig. 1. We have chosen to plot the pressure on a logarithmic scale as this accentuates the high altitude portions. Also, such a scale makes the ordinate nearly linear in the height, and thus permits a comparison of the curves on a basis of air path. Each curve has been normalized to the vertical ground counting rate of the same telescope with the lead filters removed, at Princeton. Absolute flux values may be obtained if the ground flux is known.[1]

During the period of the flights, a high counting rate telescope was used to monitor the ground intensity and, in addition, the Cheltenham ionization chamber data** were examined. No large fluctuations of intensity were present.

The curve with 1.9 cm of lead in the vertical and 22° zenith directions, and the no lead curve at 45° were obtained at Princeton (geomagnetic latitude 51°N) on November 30, 1948 (shown with heavy lines). All the other data were obtained at Camp Ripley, Minnesota (geomagnetic latitude 56°N) during the period May 22–July 4, 1948. The 7.6-cm values are an average of two flights, while all the others represent a single flight for each thickness of lead. The experiment carrying the 16.7-cm thickness of lead reached a height of 2.5 cm Hg, while the others all reached the 1.0-cm point.

The total vertical intensity curve is about the same as that obtained by Pfotzer[2] and more recently by Biehl *et al.*[3] The vertical curves with large amounts of lead resemble the data obtained by Schein,[4] showing a continual increase of intensity to the highest altitude reached (the convex upward shape is due to the logarithmic scale of pressure!). A large amount of the secondary radiation responsible for the peak in the total intensity may be removed with 1.9 cm of lead, but even the curve with this thickness shows a flat maximum at about the same point as the total intensity maximum. Data similar to this in the vertical direction have been obtained by Pomerantz[5] with filter thicknesses up to 8 cm. His results do not differ significantly from the present data.

A table of the energies necessary to penetrate the counters and the various thicknesses of Pb used in the telescopes is given in Table I.

Data on the zenith angle distribution of intensity obtained by Swann[6] with no lead filtering to pressure heights of 4 cm are in essential agreement with these results except for the horizontal intensity. Swann's horizontal value reaches about the same magnitude as the vertical intensity. In the present experiments (Fig. 1), the horizontal component is in general considerably lower than previously reported, with the exception of the measurement with 1.9 cm Pb, which increases with altitude to about the vertical value. Our other horizontal measurements with no or 7.6 cm lead (the latter from two flights) show a low value, the intensity with a 16.7-cm filter being extremely low (5 percent of the vertical). The very sharp dependence of intensity on zenith angle near the horizontal as shown

* Assisted by the joint program of the AEC and the ONR.
[1] E.g., the value $1.14 \cdot 10^{-2}$ particle/cm²/sec. given by B. Rossi (Rev. Mod. Phys. **20**, 537 (1948)). Within the accuracy of this experiment, this flux may be assumed constant, provided no severe solar disturbances or magnetic storms occurred. (See previous paper for calibration procedure.)
** Furnished through the kindness of Dr. S. E. Forbush, Carnegie Institution of Washington.

[2] G. Pfotzer, Zeits. f. Physik **102**, 23, 41 (1936).
[3] Biehl, Montgomery, Neher, Pickering, and Roesch, Rev. Mod. Phys. **20**, 360 (1948).
[4] Schein, Jesse, and Wollan, Phys. Rev. **59**, 615 (1941).
[5] M. Pomerantz, Phys. Rev. **75**, 69 (1949).
[6] Swann and co-workers, Nat. Geo. Soc. Contributed Tech. Papers, Stratosphere Series No. 2.

by the present results (see Fig. 2) would make the observed intensity very sensitive to the angle included by the telescope, or to the leveling of the instrument.

Because of the important connection between angular divergence of secondary particles and the horizontal intensity, this measurement has been repeated by T. J. B. Shanley, of this laboratory, using a telescope with a small angular operation (12:1). (See Appendix.) His results show a *large* horizontal intensity with no lead, about equal to our measured vertical value, and therefore in agreement with Swann's data. The drop of intensity with lead filtering for horizontal particles, which is in contrast to what is observed in the vertical direction at high altitude indicates that the horizontal flux is of a non-penetrating secondary nature, in agreement with an analysis presented later in this paper.

The peak total intensity, and in fact all the other curves with various filter thicknesses, shift towards greater heights as the zenith angle is increased. This effect is apparently connected with the greater air path seen at low zenith angles, as first pointed out by

TABLE I. Energies necessary to penetrate the counters and the various thicknesses of Pb used in the telescopes.

Minimum energy required by various particles to traverse telescope				Electrons[c]		
Thickness of material in counter telescope		Min. energy in Mev required to traverse[a]		Shower units of material	Energy of incoming electrons (ev)	Probability of finding no electrons under material
cm Pb	g/cm²	mesons[b]	protons			
0.29[d]	3.3[d]	15.0	38.0	0.81	7×10^7	0.07
					5×10^8	0.006
					4×10^9	0.0006
2.2	24.8	53.0	130.0	6.1	7×10^7	0.19
					5×10^8	0.04
					4×10^9	0.003
7.9	89.3	140.0	270.0	22.0	7×10^7	1.0
					5×10^8	0.7
					4×10^9	0.09
17.0	192.0	245.0	430.0	47.5	7×10^7	practically 1
					5×10^8	practically 1
					4×10^9	practically 1

[a] From curves prepared by E. P. Gross, Princeton University, December, 1947.
[b] Meson of mass 200 m_e is considered.
[c] N. Arley, *Stochastic Processes and Cosmic Radiation* (G.E.C. Gads Forlag, Copenhagen, 1943).
[d] g/cm² of Cu—obtained by considering only the counter walls.

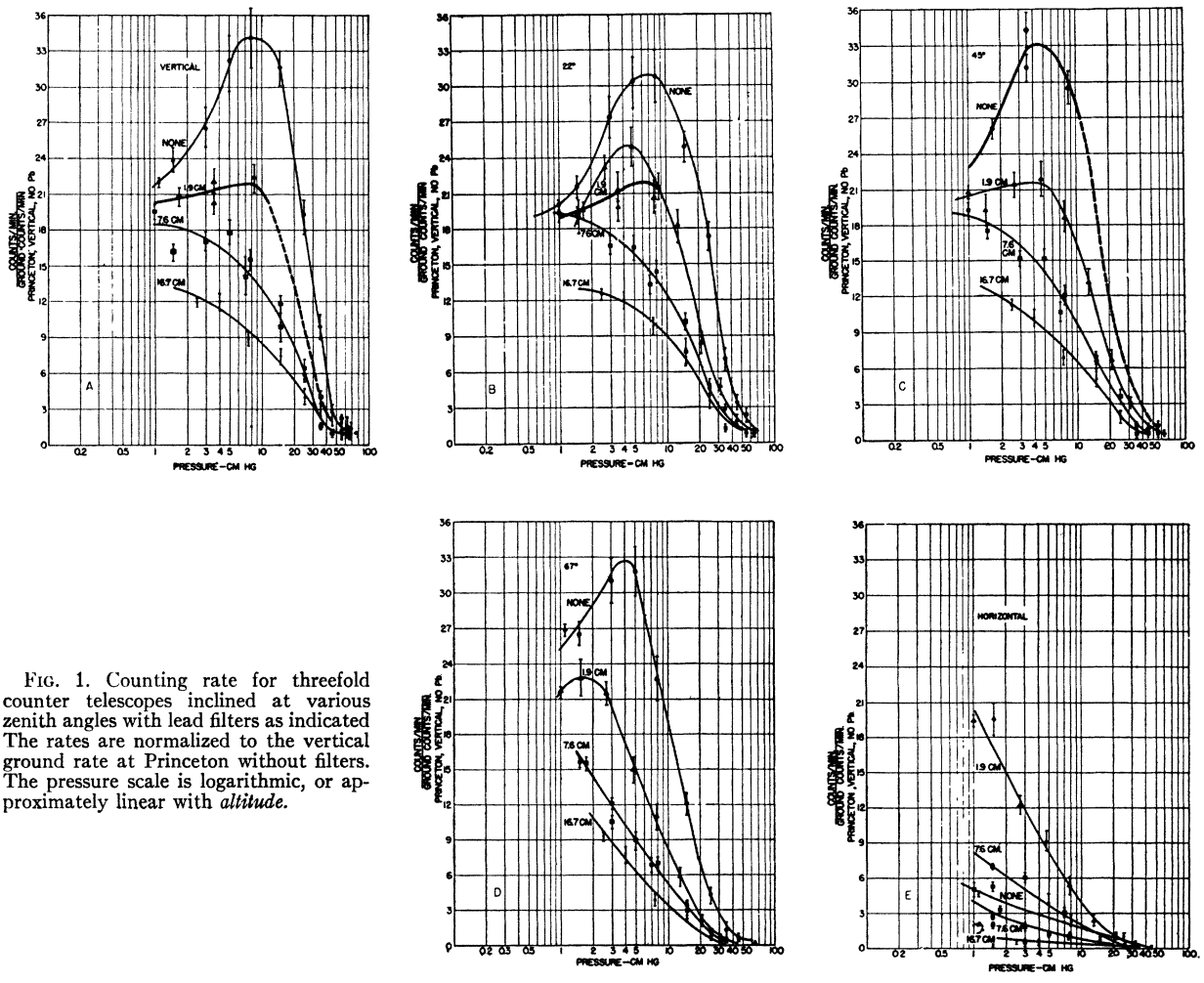

FIG. 1. Counting rate for threefold counter telescopes inclined at various zenith angles with lead filters as indicated The rates are normalized to the vertical ground rate at Princeton without filters. The pressure scale is logarithmic, or approximately linear with *altitude.*

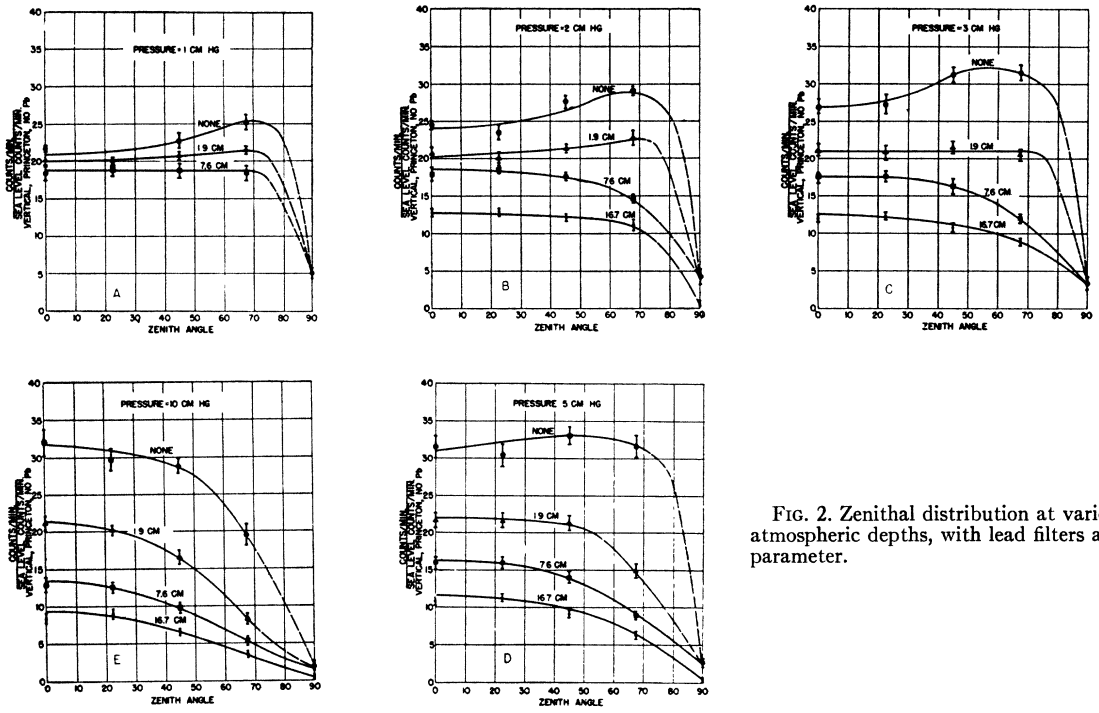

FIG. 2. Zenithal distribution at various atmospheric depths, with lead filters as a parameter.

Swann,[6] and may be expressed by the relation

$$I(p, \theta) = I(p \sec\theta, 0),$$

where I is the intensity observed at pressure p and at angle θ. If the curves at $\theta = 22\frac{1}{2}°$, 45°, and 67° of Fig. 1 are displaced along the pressure axis, they can be matched surprisingly well to the vertical curves. Then the ratio of values brought into coincidence on the pressure scale is in approximate agreement with the $\sec\theta$ as seen in Table II.

It is evident that the entire cosmic-ray absorption and multiplication process observed with vertical counter telescopes can be duplicated at lower zenith angles and correspondingly higher altitudes. This result is not surprising if the primary flux of particles is isotropic in free space. One would expect, however, a decrease in the meson intensity for low angles relative to the vertical due to decay in flight. This is a possible explanation of the fact that the curves at $67\frac{1}{2}°$ with 7.6- and 16.7-cm lead filters cannot be matched to the corresponding vertical curves by a displacement, but have a lower intensity and slightly different curvature.

TABLE II. Test of relation $I(p, \theta) = I(p, \sec\theta, 0)$.

θ	$\sec\theta$	Pressure scale ratios to match intensity-height curve at θ to value indicated
$22\frac{1}{2}°$	1.08	1.0±0.1 matched to 0°
45°	1.41	1.6±0.1 matched to 0°
$67\frac{1}{2}°$	2.60	2.2±0.1 matched to 0°
$22\frac{1}{2}°$	sec45/secθ = 1.3	1.5±0.1 matched to 45°
$67\frac{1}{2}°$	sec45/secθ = 1.9	2.0±0.1 matched to 45°

The important question as to whether the secant law implies a large degree of persistence of direction between primary and secondary particles cannot be answered without detailed analysis, and will be considered later in this paper.

The data of Fig. 1 plotted as zenith angle distributions with various lead filters at various heights are given in Fig. 2. These curves clearly show that at atmospheric pressures of 5 cm or less the unfiltered intensity at larger zenith angles is greater than the vertical. This effect is greatly reduced by a 1.9-cm lead filter, and completely removed by larger thicknesses of lead. At 1-cm pressure, a filter of about 3 cm or more gives a constant intensity with zenith angle nearly to the horizontal where the sharp drop is observed. But as the atmospheric depth is increased, the telescopes with larger lead thicknesses show a continuous decrease of intensity as zenith angle increases.

The zenith angle distributions enable one to find the total flux of particles as a function of altitude by evaluating the integral

$$J_2 = 2\pi \int_0^{\pi/2} I(\theta) \sin\theta d\theta.$$

This quantity has been plotted in Fig. 3, in which the sea-level vertical flux at Princeton was assumed to be that given by Rossi.[1] This omnidirectional flux, J_2, should be that measured by a spherical ionization chamber with walls equivalent to 2.6 g/cm² of Cu, and

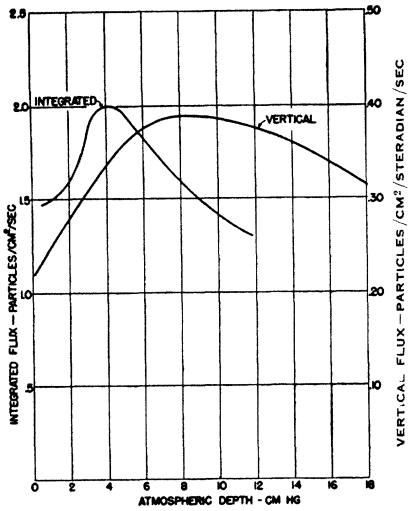

FIG. 3. The omnidirectional flux, as determined from counter telescopes without lead (2.6 g/cm² counter wall). Shown for comparison is the vertical flux (particles/cm²/sec./steradian note omission in drawing).

it can be seen from the figure that the sharp maximum at 4 cm pressure occurs at the same place as the ion chamber or single counter measurements.[7] The vertical counter telescope, on the other hand, gives the much broader maximum peaking at about 8 cm Hg.

The azimuthal distribution measured at 1.5-cm Hg height is given in Fig. 4. A nearly uniform rotation of the equipment was achieved on one of the flights with 7.6-cm lead filtering on all telescopes for a period of about four hours. The data have been summed in each 45° sector at zenith angles of 45°, 67½°, and 90°, and are entirely consistent with an isotropic primary flux. A similar result was obtained by Swann without lead filters,[6] although at lower altitude where secondary particles are more numerous.

II. INTERPRETATION

It is probable that even at the heights reached by high altitude balloons an appreciable fraction of the primary rays have undergone absorption in the atmosphere, and have multiplied into secondary rays which may diverge in direction from the primary rays. The angular divergence of secondaries may obscure an azimuthal asymmetry measurement at fixed zenith angle, and the multiplication and absorption processes give an erroneous relation between primary intensities at different zeniths because of the changing air path. The horizontal intensity observed in these experiments indicates that the angular divergence of penetrating secondaries is not large, but the multiple production of forward-moving secondaries is shown even at the highest altitudes reached by the increase of intensity with zenith angle at angles as large as 70°.

To give a more quantitative meaning to these experiments, several kinds of assumptions about the angular divergence and multiplicity of secondary particles have been made, and in each case the expected zenithal distribution was calculated for comparison with experiment.

An isotropic primary flux of intensity I_0 particles/sec./cm²/per steradian was assumed. These particles are absorbed in the atmosphere according to the relation

$$I' = I_0 e^{-\mu x \sec\psi}, \tag{1}$$

where x is the atmospheric depth in g/cm², μ the absorption coefficient in cm²/g, and ψ the zenith angle of the ray. Secondary particles are produced by a catastrophic event with an angular distribution in the laboratory system given by a function, $f(\theta_{12})$, of the angle θ_{12} between the primary and secondary directions. Consider those secondaries produced by a primary entering an atmospheric layer of thickness dx (see Fig. 5) at zenith angle ψ and azimuth ϕ, where $\phi=0$ is in the plane passing through the vertical and the direction of observation. The layer dx is at depth x and the secondary particles travel at a zenith angle θ toward the point of measurement located at atmospheric depth y. The secondary particles are also assumed to be absorbed exponentially with coefficient ν according to the relation

$$I'' = I_0'' e^{-\nu|y-x|\sec\theta}. \tag{2}$$

The multiplicity N (number of secondaries/primary) is given by

$$N = 2\pi \int_0^\pi f(\theta_{12}) \sin\theta_{12} d\theta_{12}. \tag{3}$$

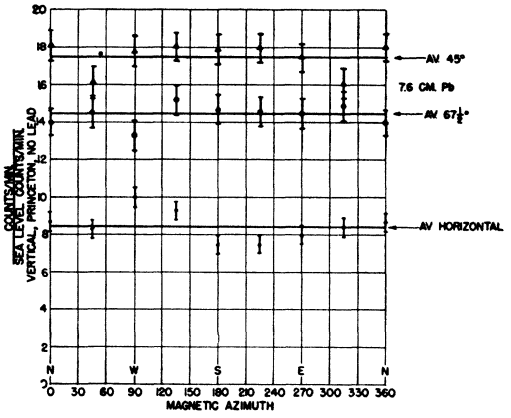

FIG. 4. The azimuthal distribution at about 1.5 cm Hg atmosphere depth with 7.6-cm Pb filter, at 45°, 67½°, and 90° zenith angles.

The intensity $I(y, \theta)$ is then given by the sum of primaries and secondaries reaching the depth y at zenith angle θ:

$$I(y,\theta) = I_0 e^{-\mu y \sec\theta} + \mu I_0 \sec\theta \int e^{-\mu x \sec\psi} \times \sin\psi e^{-\nu|y-x|\sec\theta} f(\theta_{12}) d\psi d\phi dx. \tag{4}$$

[7] Millikan Neher, and Pickering, Phys. Rev. **61**, 397 (1942).

Equation (4) includes both upward and downward moving particles if the absolute value of the secondary path length, $y-x$, is preserved in the integration.

Consider three kinds of secondary distributions:

Case 1: $f(\theta_{12})=0$.

This corresponds to the experimental condition that the secondaries have been completely absorbed by filters in

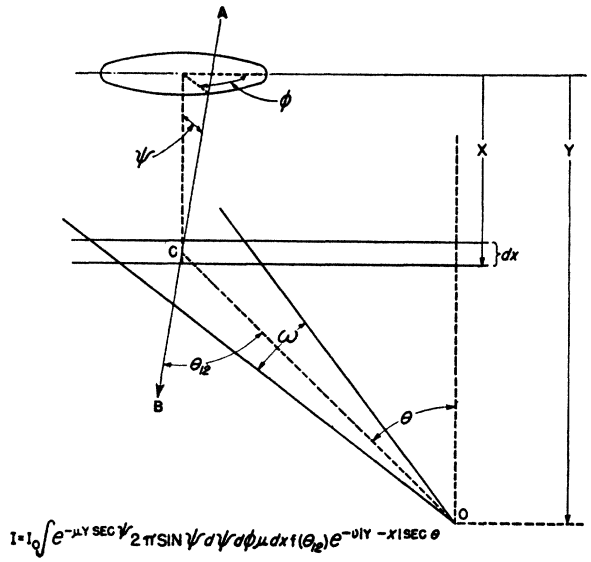

FIG. 5. The geometry considered in Eq. (4). AB is the path of a primary ray, making an angle ψ with the vertical and an angle ϕ, in the horizontal plane, with the plane through the vertical and the direction of observation CO. Secondaries produced in a layer dx at atmospheric depth x with an angle of divergence θ_{12} from AB are observed at 0 at a depth y by a telescope of solid angle ω at a zenith angle θ.

the apparatus, and that only the primary rays are detected, their intensity being given by the first term of Eq. (4).

Case 2: $f(\theta_{12})=0$ when $\theta_{12}\neq 0$, $f(\theta_{12})=N$ when $\theta_{12}=0$ which has the physical meaning that N secondary particles continue in the direction of the primary after the absorption of the latter. (These secondaries are detected as individual particles.)

Case 3: $$f(\theta_{12})=c(1+\cos\theta_{12})^n. \quad (5)$$

This gives a distribution of secondaries with an adjustable angular divergence. For $n=1$, the intensity at $\theta=\pi/2$ is 50 percent of that at $\theta=0$, but at this same angle drops to about 5 percent for $n=4$. A large horizontal and upward flux results from so broad an assumed distribution.

In Fig. 6 are plotted the calculated depth-zenith angle distribution in Case 1, Eq. (4) being reduced to:

$$I(y,\theta)=I_0e^{-\mu y\ \sec\theta}. \quad (6)$$

For comparison with experiment, one observes that the vertical intensity at 1 cm pressure where secondaries are not numerous is reduced very little by a 7.6-cm lead filter. At greater depths where secondaries are more numerous, the same filter has a very large effect. Thus this 7.6-cm filter seems to approximate the ideal filter of Case 1, which is supposed to select only primary particles. The observed intensities using this filter agree best with an absorption coefficient μ of 1/275 cm^2/g and appear to be consistent with the interpretation that these particles are primary rays. However, the possibility of equally *penetrating* secondaries produced with a multiplicity near unity is not ruled out. Also, the observed horizontal flux at 10-cm Hg depth with the 7.6-cm Pb filter is too high to consist of primary particles, whose intensity, as given by Eq. (6), would be very low.

Case 2, in which N secondaries continue in the direction of the primary ray after the catastrophic absorption of the latter, results in a simplification of Eq. (4) to

$$I(y,\theta)=I_0e^{-\mu y\ \sec\theta}+\mu N I_0\sec\theta\int_{x=0}^{y}e^{-\mu x\ \sec\theta}e^{-\nu|y-x|\ \sec\theta}dx$$

$$=I_0\left\{\left[1+\frac{\mu N}{\nu-\mu}\right]\exp(-\mu y\sec\theta)-\frac{\mu N}{\nu-\mu}\exp(-\nu y\sec\theta)\right\}. \quad (7)$$

Formula (7) is plotted in Fig. 7.

The best fit with the unshielded telescope data (see Fig. 2) at $y=13.5$ g/cm^2 and $y=135$ g/cm^2 is obtained with N close to 3, $\mu=1/275$ cm^2/g and ν between 1/100 and 1/150 cm^2/g.

If the effect of the earth's curvature is taken into account at the highest altitude, the calculated horizontal flux I/I_0 is raised both in Case 1 and Case 2 to about 0.3, in agreement with experiment at 13.5 g/cm^2. This point is discussed more fully in a later section.

Equation (7) has been compared with the *unshielded* telescope data, as the effects of lead absorbers on secondary particles at various points in their range is difficult to estimate. The exponential, rather than the range type of absorption was chosen for secondaries because of their probable distribution in energy and nature.

Assume now a wide angular divergence for secondaries given by Eq. (5) with $n=1$. The multiplicity of secondary production in terms of c is given by

$$N=2\pi c\int_0^{\pi}(1+\cos\theta_{12})\sin\theta_{12}d\theta_{12}, \quad (8)$$

which leads to the normalization $c=N/4\pi$. Using the relation

$$\cos\theta_{12}=\cos\theta\cos\psi-\sin\theta\sin\psi\cos\phi,$$

the angles being defined in Fig. 5, the ratio of observed

to primary flux is given by the equation

$$I/I_0=e^{-\mu y\ \sec\theta}+(\mu N/4\pi\cos\theta)\int\exp[-\mu x\sec\psi]\times\exp[-\nu|y-x|\sec\theta]\sin\psi(1+\cos\theta\cos\psi-\sin\theta\sin\psi\sin\phi)d\psi d\phi dx. \quad (9)$$

The integration is first carried out with respect to the azimuth θ over a 2π-interval. The integration with respect to the atmospheric depth x is carried out from $x=0$ to $x=y$ for downward moving secondaries, and from $x=y$ to $x=y_0$ for upward moving secondaries, where y is the depth of the point of observation and y_0 is the lower limit of the atmosphere. For upward particles, the distribution function $f(\theta_{12})$ must be replaced by $f(\pi-\theta_{12})$.

The downward moving flux, including primaries, is given by the relation

$$I_{\text{down}}/I_0=\exp(-\mu y\sec\theta)+\frac{N}{2}(I_1+I_2), \quad (10)$$

where

$$I_1=[-E_i(-\mu y)][(\mu/\nu)^3\cos^3\theta+(\mu/\nu)^2\cos\theta-(\mu/\nu)\mu y-(\mu/\nu)^2\mu y\cos^2\theta+\tfrac{1}{2}(\mu/\nu)(\mu y)^2\cos\theta]-[E_i(\nu y\sec\theta-\mu y)][e^{-y\nu\ \sec\theta}(-(\mu/\nu)^2\cos\theta-(\mu/\nu)^3\cos^3\theta)]+e^{-\mu y}[\mu/\nu+(\mu/\nu)^2\cos^2\theta+\tfrac{1}{2}(\mu/\nu)\cos\theta-\tfrac{1}{2}(\mu/\nu)\mu y\cos\theta],$$

$$I_2=-e^{-\nu y\ \sec\theta}\{\log_e[1-(\nu\sec\theta/\mu)]\times[(\mu/\nu)^3\cos^3\theta+(\mu/\nu)^2\cos\theta]+\mu/\nu+\tfrac{1}{2}(\mu/\nu)\cos\theta+(\mu/\nu)^2\cos^2\theta\}.$$

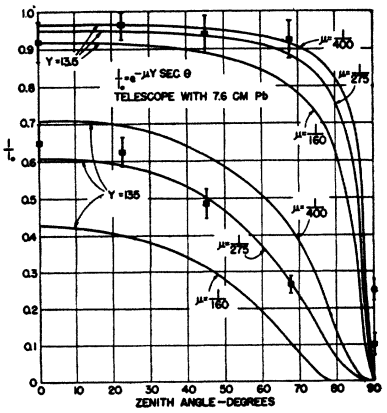

FIG. 6. Plot of $I/I_0=e^{-\mu y\ \sec\theta}$ *vs.* zenith angle θ, for absorption coefficients of $\mu=1/400$, $1/275$, and $1/160$ cm²/g, respectively, at atmospheric depths given by $y=13.5$ and 135 g/cm². The squares represent the experimental data obtained under 7.6 cm Pb at these two atmospheric depths.

The upward flux is

$$I_{\text{up}}/I_0=\frac{N}{2}\{[-E_i(-\mu y)]\times[-(\mu/\nu)^3\cos^3\theta-(\mu/\nu)^2\cos\theta-(\mu/\nu)\mu y-(\mu/\nu)^2\mu y\cos^2\theta-\tfrac{1}{2}(\mu/\nu)\mu^2y^2\cos\theta]+[-E_i(-\{\mu y+\nu y\sec\theta\})]e^{\nu y\ \sec\theta}\times[(\mu/\nu)^2\cos\theta+(\mu/\nu)^3\cos^3\theta]+e^{-\mu y}[\mu/\nu+(\mu/\nu)^2\cos^2\theta-\tfrac{1}{2}(\mu/\nu)\cos\theta+\tfrac{1}{2}(\mu/\nu)\mu y\cos\theta]\}. \quad (11)$$

For the special case $\theta=90°$, these expressions reduce to

$$I/I_0=\frac{N\mu}{2\nu}\{e^{-\mu y}-\mu y[-E_i(-\mu y)]\}, \quad (12)$$

which includes the contributions to the horizontal flux from both directions. E_i is the integral-exponential function, tabulated, for example, in the W.P.A. Mathematics Tables.***

The contributions to the observed intensity from upward and downward moving particles are listed in Table III, and the total intensity is plotted in Fig. 8 for a range of values of θ at atmospheric depths $y=13.5$ and $y=135$ g/cm². In one case it was assumed $N=3$, $\mu=1/275$, and $\nu=1/125$, and in a second case $N=10$, $\mu=1/275$, and $\nu=1/60$. The consequences of the assumed distribution $f(\theta_{12})=c(1+\cos\theta_{12})$ are, as shown in Fig. 8, a high horizontal particle flux, and a vertical intensity at $y=135$ g/cm² which is *less* than that at $y=13.5$ g/cm². The latter fact is in complete disagreement with experiment (e.g., the Pfotzer maximum). The over-all intensity for $N=10$ is too high at 13.5 g/cm² atmospheric depth. However, for $N=3$, the

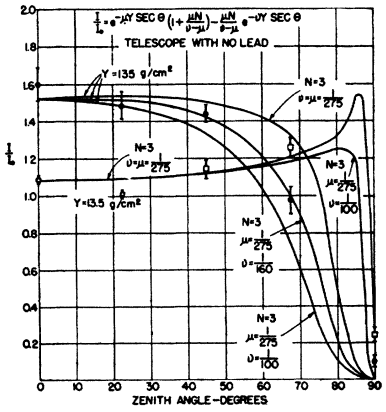

FIG. 7. Zenithal distribution of particles under the assumption of a sharply collimated forward burst of multiplicity N. Ordinate ratio of total flux to incident primary flux.

*** *Tables of Sine, Cosine, and Exponential Integrals* (U. S. Works Projects Administration, 1940) Vol. 2.

horizontal intensity is about correct to agree with our most recent measurement, as well as that of Swann.[6] Best agreement with the experimental results would evidently be obtained by a production event combining Case 2 and Case 3, that is, a penetrating bundle of forward moving particles (mesons?) and a wide angle burst of low energy particles (electrons, nucleons?), which can be absorbed in a few cm of lead.

In all the computations so far in this paper, the earth's atmosphere was assumed to be flat, corresponding to an earth of infinite radius. The effect of the finite curvature at high altitude and low zenith angles is to shorten the air path, and to make its value finite even in the horizontal direction. If $\rho(r-r_e)$ is the atmospheric density at a radius r, where r_e is the earth's radius, the total air mass in the vertical direction above a point $r=r_0$ is

$$m_0=\int_{r_0}^{\infty}\rho(r-r_e)dr. \tag{13}$$

The air mass seen from the point r_0 obliquely at a zenith angle θ is given by

$$m=\int_{r_0}^{\infty}\frac{\rho(r-r_e)rdr}{(r^2-r_0^2\sin^2\theta)^{\frac{1}{2}}}. \tag{14}$$

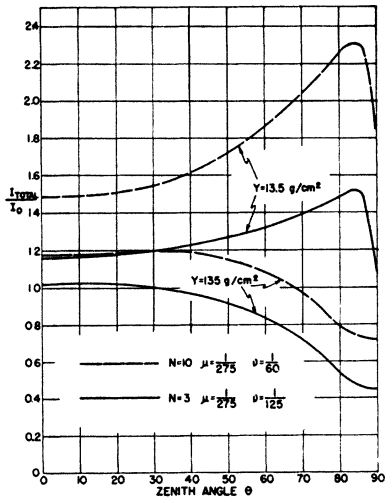

FIG. 8. Zenithal distribution of particles at two atmospheric depths calculated from an assumed wide-angle burst of secondaries. The lack of increase with depth for vertical particles (Pfotzer maximum) is in disagreement with experiment for both $N=3$ and $N=10$. For $N=10$ the over-all intensity at 13.5 g/cm² depth is too high. The horizontal intensity at this depth for $N=3$ agrees with our most recent measurement, and the data of Swann for unshielded telescopes. These results suggest penetrating *forward* moving particles and a wide-angle burst of low energy particles as the typical production event.

If we take for ρ the function $\rho=\rho_0\exp[-\alpha(r-r_e)]$ which corresponds to the earth's atmosphere with r and r_e in kilometers and $\alpha=0.12$ and make the substitution $\delta=r-r_e$, we find for the ratio P of the vertical-to-the-oblique air mass, the value

$$m/m_0=P=0.12(r_0/2)^{\frac{1}{2}}\int_0^{\infty}\frac{e^{-0.12\delta}d\delta}{((r_0/2)\cos^2\theta+\delta)^{\frac{1}{2}}}. \tag{15}$$

In this expression, we have neglected δ in comparison with r_0 because of the rapid falling off of the integrand with δ. In the case $r_0/2\cos^2\theta\gg\delta$ corresponding to values of θ between 0 and 70°, P reduces to $\sec\theta$. The behavior of P as compared with $\sec\theta$ is given in Table IV. P is insensitive both to the atmospheric depth and the value of α in the atmospheric density function. It is not possible to take account of this air path correction exactly in the type of secondary angular distribution assumed in Case 3, but because of the weak directional correlation between primary and secondary particles the effect on the calculations is very small. However, in Cases 1 and 2 the correction may be applied. The actual air path at $\theta=90°$ and at an atmospheric depth of 13.5 g/cm² is the same as the secant law air path at 88°. Accordingly, I/I_0 (secant law, 88°)$=I/I_0(90°)$. This correction brings the calculation into apparently good agreement with the horizontal measured value in both Case 1 and Case 2.

TABLE III. Directional distribution of particles, assuming widely diverging secondaries $[f(\theta_{12})=c(1+\cos\theta_{12})]$.

Zenith angle degrees	Particle flux I/I_0: $N=3$, $\mu=(1/275)$ cm²/g, $\nu=(1/125)$ cm²/g, Atmospheric depth 13.5 g/cm² Down	Up	135 g/cm² Down	Up	$N=10$, $\mu=(1/275)$ cm²/g, $\nu=(1/60)$ cm²/g, Atmospheric depth 13.5 g/cm² Down	Up	135 g/cm² Down	Up
0	1.05	0.11	0.98	0.04	1.25	0.24	1.10	0.08
40	1.05	0.17	0.90	0.07	1.26	0.35	1.06	0.13
70	1.06	0.32	0.59	0.14	1.42	0.61	0.73	0.25
80	1.06	0.42	0.35	0.18	1.52	0.74	0.49	0.30
85	1.02	0.49	0.27	0.20	1.49	0.82	0.41	0.33
90	0.57	0.57	0.23	0.23	0.91	0.91	0.36	0.36

III. CONCLUSIONS

The results of these experiments are in accord with a mean free path for primary rays in air of 275 g/cm², with a rather large uncertainty due to the effects of penetrating secondaries. The zenithal distribution curves considered in the light of an analysis of secondary particle production indicate sharply forward moving secondaries of multiplicity about 3 and with a mean

TABLE IV. Comparison of air paths. Flat atmosphere (secant law) *vs.* curved atmosphere.

Zenith angle degrees	Secant θ	Relative air path—P
0	1.0	1.0
45	1.41	1.41
70	3.08	3.00
80	5.75	5.25
85	11.46	9.45
89	57.1	25.4
90	∞	27.0

free path of from 100 to 150 g/cm². These conclusions are supported by other recent results[8] which indicate that the east-west asymmetry is preserved to a large extent at considerable atmospheric depths. The horizontal flux is a very sensitive measure of the angular divergence of secondary rays. A large angular divergence produces a large horizontal and upward moving flux. The experimental results indicate that the widely divergent particles responsible for the horizontal flux have low energy and are easily observable as such.

The theoretical assumptions are certainly an oversimplified picture of the complex cosmic-ray processes at the top of the atmosphere. Nevertheless, these results show that the effects of the atmosphere at 13 g/cm² depth on a projected study of the primary directional asymmetry are not large. The small effect of lead absorbers on vertical rays at this depth rules out any appreciable number of electrons or photons of low energy trapped in the earth's magnetic field above the atmosphere. The multiplication of primaries into secondaries is noticeable as an increase of intensity at large zenith angles where the air path is larger, but lead filters of a few cm thickness reduces the apparent multiplicity to near unity. Finally, the analysis shows that those secondary rays are sharply collimated, and therefore asymmetry measurements should not be in error due to secondary effects.

ACKNOWLEDGMENT

The writers wish to express their indebtedness to Professor J. A. Wheeler, who first interested the senior author (J. W.) in this problem, and who has provided support and encouragement at every step in the way. Thanks are due to Mr. Kenneth Ford for evaluating some of the integrals.

APPENDIX ON REDETERMINATION OF HORIZONTAL INTENSITY WITH NO LEAD FILTER

In view of the anomalous result obtained for the horizontal intensity with no lead filter (see Fig. 1E), a threefold horizontal Geiger counter telescope was sent to 78,000 feet, counting rate and pressure being radioed to the ground by an f-m telemetering system. The counters had an effective length of 12 inches, one inch diameter, and were filled with a mixture of argon and ethelyne. End counters were separated by 12 inches, giving an effective angular opening of about 4°. Counter pulses were fed into a threefold Rossi coincidence circuit with a resolving time of 2×10^{-5} sec. The vertical ground counting rate of the counter telescope was 1.986±0.021 counts per minute. This apparatus was launched from Princeton on May 14, ascended to an altitude of 2.3±0.2 cm Hg (~78,000 feet) at an average rate of about 800 feet per minute. It remained at this altitude for 153 minutes, then descended at approximately the same rate and was recovered. Radio contact with the equipment was maintained throughout the flight. After the flight the vertical ground counting rate was 1.90±0.04 counts per minute, the decrease being attributable to a considerable misalignment of the counter telescope when the equipment struck the ground.

TABLE V. Counting rate *vs.* pressure in cm Hg. Each counting rate shown in the second column is an average value over the corresponding pressure range indicated in the first column, corrected for counter inefficiency. The third column gives the ratio of the actual counting rates to the ground counting rate of the telescope in a vertical position. Data marked with an asterisk was obtained during the descent, all other data during the ascent.

Pressure range in cm Hg	Average counting rate, counts per min.	Normalized counting rate
21.2–12.7	6.8±0.9	3.4±0.5
12.7–6.8	11.2±0.8	5.6±0.4
6.8–5.6	25.0±2.0	12.6±1.0
5.6–4.1	33.4±2.0	16.8±1.0
4.1–3.1	37.2±2.0	18.7±1.0
3.1–2.5	42.5±2.1	21.4±1.1
2.5–2.1	42.84±0.25	21.57±0.13
*2.5–3.4	39.6±2.2	20.0±1.1
*3.4–4.4	33.4±2.0	16.8±1.0
*4.4–5.9	30.4±1.9	15.3±1.0
*5.9–7.1	22.6±2.0	11.4±1.0
*7.1–12.1	18.6±1.1	9.4±0.6

The results are given in Table V, corrected for counter inefficiency. No shower correction was applied. The correction for accidental threefold coincidences is negligible.

These results show that the no lead horizontal counting rate exceeds all horizontal counting rates with lead filters between the counters. We here obtain 21.57 counts/min. at 2.2 cm Hg with no lead, compared to 14.6 counts/min. at the same altitude with a 1.9-cm Pb filter (see Fig. 1e).

Comparison of counting rate at 2.1 cm Hg with various thicknesses of lead absorbers give an absorption coefficient of 1/56 (gram/cm²)$^{-1}$ for horizontal particles if they are absorbed exponentially. Fifty-six grams/cm² is the range in lead of 200-Mev protons. The exponential absorption coefficient in lead for the vertical flux is 1/274 (gram/cm²)$^{-1}$ at the same altitude. It is clear that most of the horizontal praticles are secondaries.

[8] Stroud, Schenck, and Winckler, Phys. Rev., preceding paper.